

# Si-SiO<sub>2</sub> interface band-gap transition: effects on MOS inversion layer characteristics

S. Markov<sup>\*†</sup>, P. Sushko<sup>‡</sup>, S. Roy<sup>\*</sup>, C. Fiegna<sup>†</sup>, E. Sangiorgi<sup>†</sup>, A. Shluger<sup>‡</sup>, and A. Asenov<sup>\*</sup>

<sup>\*</sup>EEE Dept., Univ. of Glasgow, Glasgow G12 8LT, United Kingdom

<sup>†</sup>ARCES-IUNET, Univ. of Bologna, v. Venezia 52, Cesena 47023, Italy

<sup>‡</sup>Dept. Physics and Astronomy, Univ. College London, WC1E 6BT, United Kingdom

e-mail: s.markov@elec.gla.ac.uk

## INTRODUCTION

The change of the atomic structure at the Si-SiO<sub>2</sub> interface leaves additional electronic states, energetically aligned closer to the Si conduction band, in the first 2 – 6 Å of the SiO<sub>2</sub> away from the interface [1], [2], [3], [4]. This implies a gradual transition of the band-gap at the SiO<sub>2</sub> side, as shown on Fig. 1 from [2]. Recently, we studied the impact of this transition on the metal-oxide-semiconductor (MOS) inversion layer characteristics [5], simulating linear transition of the band-gap, similarly to earlier studies [6], [7]. For the first time here, MOS inversion layer quantisation, capacitance and tunnelling characteristics are analysed for a realistic band-gap transition, derived from first principles simulations of the Si-SiO<sub>2</sub> interface.

## SIMULATION APPROACH AND RESULTS

This study is based on a 1-D self-consistent solution of the Poisson and Schrödinger equations, using a modified version of Schred 2.0 solver [8], as in [9] and [5]. Further modifications allow us to incorporate the interface band-gap profile from Fig. 1. We have re-scaled the values extracted from Fig. 1, since this profile results from density-functional theory, which is known to underestimate the band-gap, compared to experimentally observed values [4]. Since non-linear features of the transition are preserved, we confront the results obtained from this transition profile, with simulations of a linearly graded band-gap transition in the range of 0.2 – 0.6 nm. The simulated MOS structures has a SiO<sub>2</sub> dielectric of thickness in the range of 1.0 – 1.8 nm, and a p-Si (100) substrate, uniformly doped to  $2 \times 10^{18} \text{ cm}^{-3}$ . Metal gate with a 4.1 V work function is assumed, to avoid poly-Si depletion.

Conduction band profile and electron density distribution are compared on Fig. 2, for three different interface band-gap transition profiles. Although the full band-gap for the realistic profile extracted from Fig. 1 develops in 0.5 nm, the electrostatic effects correspond to a linear transition of 0.6 nm. The effectively wider potential well corresponding to the realistic profile lowers the ground states for both 2-fold and 4-fold degenerate Si valleys, as shown on Fig. 3, and leads to more dramatic redistribution of carriers (lower graphs on Fig. 3). Figure 4 shows an increase of gate capacitance due to the band-gap transition. The enhancement is strongest for the realistic profile, due to the strongest penetration of the corresponding wave-functions (lower part of Fig. 2). Similarly, tunnelling is mostly increased for the realistic profile, due to the thinnest tunnelling barrier for the energy range of interest - Fig. 4. Figures 5 and 6 show the relative effect of band-gap transition on quantisation, tunnelling and gate capacitance. The isolated points show where the realistic profile stands with respect to the trend of increasing the transition width of a linear profile.

We conclude that not so much the total width, but the exact profile of the band-gap transition in the first few Å is deterministic for the impact of Si-SiO<sub>2</sub> transition on MOS inversion layer characteristics.

## REFERENCES

- [1] D. A. Muller *et al*, Nature **399**, 758 (1999).
- [2] C. Kaneta *et al*, Microelectr. Engineering, **48**, 117 (1999).
- [3] T. Hattori *et al*, Appl. Surf. Sci. 212-213 (2003) 547.
- [4] F. Giustino, A. Pasquarello, Surface Sci. **586**, 183 (2005).
- [5] S. Markov *et al*, Proc.Int.Conf.SISPAD'07,to be published
- [6] F. Stern, Solid State Commun. **21**, 163 (1977).
- [7] H. Watanabe *et al*, IEEE Trans.Electr.Dev. **53**,1323,(2006)
- [8] D. Vasileska, Z. Ren SCHRED 2.0 User Manual.
- [9] N. Barin *et al*, Proc. ESSDERC, 169-172 (2004).

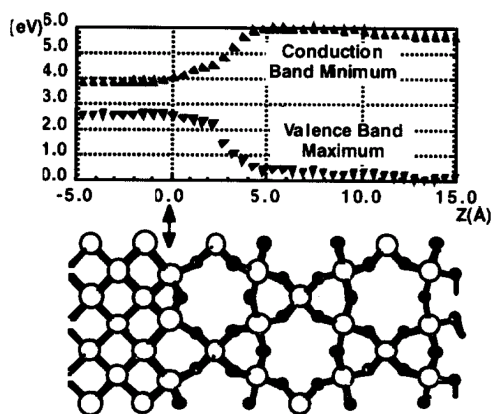


Fig. 1. Non-abrupt band-gap transition at the Si-SiO<sub>2</sub> interface (top), corresponding to the *ab-initio* simulated atomic structure of the interface (bottom), from Kaneta et al. [2].

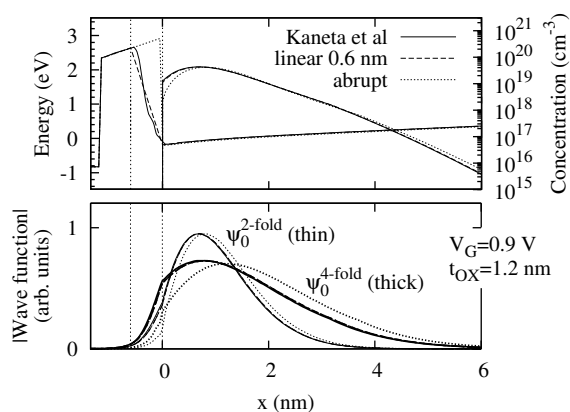


Fig. 2. Conduction band profile and electron density (upper) for three different band profiles at the interface - abrupt, linearly graded, and the band profile extracted from Fig. 1. Normalised wave functions (modulus) corresponding to the lowest sub-bands in the 2- and 4-fold valleys (lower).

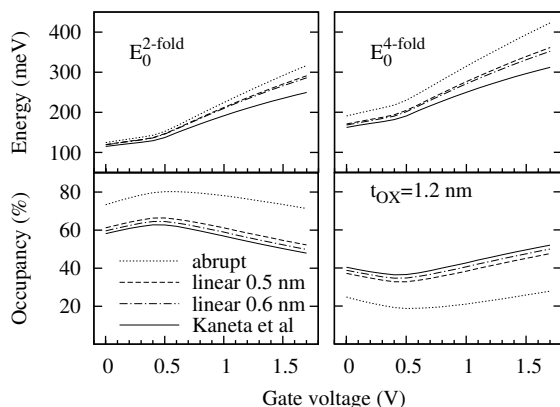


Fig. 3. Sub-band energy and sub-band occupancy (percentage of the total inversion charge density) dependence on gate voltage, for the three different interface band-gap transition profiles, as on Fig. 2, at a given oxide thickness  $t_{OX}$ .

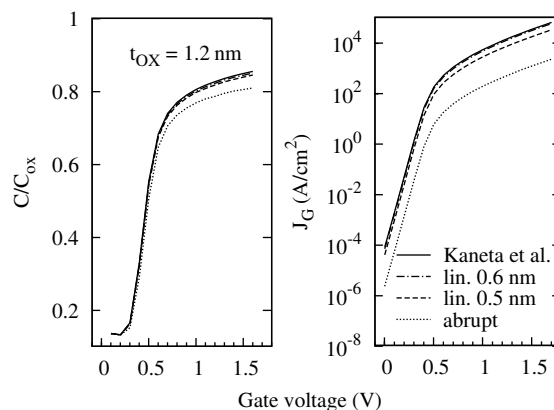


Fig. 4.  $C - V$  (left) and  $J_G - V$  (right) characteristics of the structure, for the three different band-gap transition profiles, as on Fig. 2, at a given oxide thickness  $t_{OX}$ .

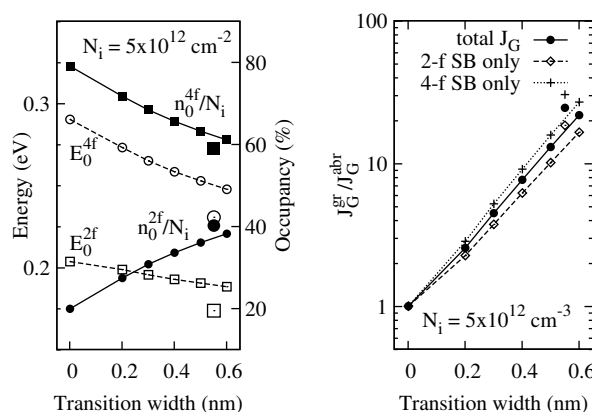


Fig. 5. Sub-band energy and occupancy (left), and direct tunnelling current (right) dependence on transition width for a constant inversion charge,  $N_i$ . The non-connected points correspond to the band-gap transition profile from Fig. 1. These results are independent of the simulated oxide thickness.

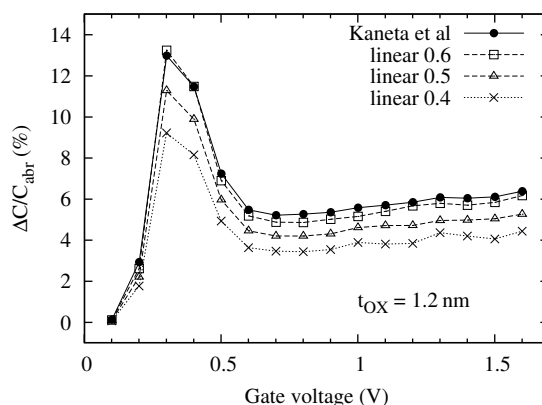


Fig. 6. Gate capacitance relative difference, with respect to abrupt interface, for various linear transition widths and for the profile from Fig. 1, at a given oxide thickness,  $t_{OX}$ .